Dust Particle Trajectories in Aircraft Radial Turbines

W. B. Clevenger* and W. Tabakoff†
University of Cincinnati, Cincinati, Ohio

This paper presents the results of analytical and experimental studies of the trajectories that atmospheric dust particles follow as they move through a radial turbine. A dimensionless parameter is derived which can be used during preliminary design analysis to indicate the sizes of particles that will be most damaging to the turbine. The study reveals several internal surfaces that will be more severely eroded because most particles entering the turbine will strike them. A moderate amount of erosion can be expected near the end of the scroll and on the last few nozzle passages near the end of the scroll. All particles greater that 42μ will strike these surfaces. A severe erosion problem occurs on the nozzle trailing edges, because particles greater than 2-3μ will not penetrate the rotor. These particles are pushed outward by centrifugal forces where they bounce off the nozzle trailing edges. Particles greater than 21μ have enough inertia to overcome the centrifugal force and these particles enter the rotor. After striking the rotor with a perpendicular impact, they also travel outward to the nozzle trailing edges.

Nomenclature

A = area, m^2
C_D = drag coefficient
D = diameter, m
$\mathbf{e}$ = unit vector
F = centrifugal force, N
g = acceleration of gravity, m/sec^2
m = mass, kg
P = particle diameter limit parameter
r = radius, m
S = characteristic length, m
t = time, sec
$\mathbf{V}$ = gas velocity with respect to the particle, m/sec
w = gas velocity with respect to the rotating reference frame, m/sec
X = similarity multiplying factor
z = axial distance, m
α = angle of meridional velocity vector with respect to radial direction, shown in Fig. 5, deg.
β = angle of velocity vector with respect to meridional velocity, shown in Fig. 5, deg.
$\delta/\delta t$ = rate of change with respect to the rotating reference frame, 1/sec
θ = angular position, deg.
ρ = density, kg/m^3
σ = angular position of the vertical axis, deg
ϕ = angular position of the turbine's axis with respect to the gravitational horizontal, deg
ω = rotational speed, rad/sec

Subscripts

cr = property evaluated at critical condition
g = gas property
p = particle property
r = component in the radial direction
θ = component in the tangential direction
SiO_2 = property associated with silicon dioxide particle
Std = term evaluated at standard sea level conditions
tip = term evaluated at rotor tip radius
u = component in the tangential direction
x = property associated with another particle
z = component in the axial direction

Presented as Paper 75-844 at the AIAA 8th Fluid and Plasma Dynamics Conference, Hartford, Conn., June 16-18, 1975; submitted June 30, 1975; revision received Nov. 25, 1975. This research was sponsored by NASA Grant 36-004-55, Lewis Research Center, Cleveland, Ohio. The authors wish to acknowledge the helpful discourse provided by H. Rohlik in the solution of this problem.

Index categories: Aircraft Subsystem Design; Multiphase Flows.

*Senior Analytical Engineer, Pratt and Whitney Aircraft, East Hartford, Conn. Formerly associated with the University of Cincinnati. Member AIAA.

†Professor of Aerospace Engineering. Associate Fellow AIAA.

Introduction

In recent times, the problem of particle erosion has become important because of the significant decreases in the rated operating performance and lifetimes of gas turbine engines used in dusty environments. The most significant effects of erosion have been observed on aircraft operated at low altitudes and remote landing fields where a significant number of particles have been ingested into the engine. Although these aircraft have main engines which utilize axial flow turbines, most of them have auxilary radial inflow turbines which are used as power sources for special devices and cabin pressurization systems.

Such radial inflow turbines potentially are subject to excessive rates of erosion when operated in dusty environments. The high rates occur because of the unique characteristic of the radial inflow turbine which concentrates particles so that most of them strike relatively small surface areas within the turbine. In addition, centrifugal forces acting on dust particles that enter the rotor prevent these particles from passing through the turbine. This phenomenon, coupled with the concentration effect, leads to much higher rates of erosion than are experienced normally on surfaces of axial flow turbines.

There have been several reports published which give results that will be useful for comparison purposes in this paper. Montgomery and Clark[1] describe a test program that was performed to relate the decrease in radial turbine engine operating lifetime to the amount and size of particles that enter the engine. These studies indicated that particles as small as 2-3 μ still can be expected to cause a serious decrease in the engine operating lifetime.

The results of an experimental effort to study erosion in radial turbines have been reported by Shoemaker and Shumate.[2] The study describes several design modifications that were performed to reduce the seriousness of the erosion that occurred. The authors indicated that the modifications were only slightly successful.

Several papers have concentrated on the effect of particle motion in flowfields that are treated as two-phase flows.[3,4] The information from such an approach is useful, but the problem becomes quite complicated with the addition of variable particle sizes and densities, and the realization that each species of particle must satisfy the continuity, momentum, and energy equations. In addition, this type of solution

does not provide information about the trajectories, which is required if conclusions about the locations and magnitudes of erosion are to be considered.

Other authors present results for cascades and annular flow geometries, respectively.[5,6] The analytical parts of these reports result from the integration of the equations of motion of a particle superimposed on the flowfield. This same method will be used in the analytical work that is presented here.

The trajectories given in this paper are presented in terms of silicon dioxide (SiO_2) particles having various diameters. A previous work presents a similarity parameter that can be used to relate particles of different sizes and materials that will follow the same trajectories in equivalent gas flowfields.[7] By using this similarity concept, the trajectories of SiO_2 particles can be used to predict the trajectories of a wide range of other particle materials.

Gas Flow Analysis

The analysis of particle trajectories in a fluid requires the solution of the fluid flowfield and also the equations of motion of a particle immersed in the fluid. A typical radial inflow turbine was selected as a model for the results presented here. Figure 1 illustrates the general configuration of the turbine model which had an equivalent flow rate of 0.0220 kg/sec, with a total-to-total efficiency of 88%. The equivalent rotating speed was 30,800 rpm. Figure 2 indicates the velocity diagrams that describe the direction and magnitude of the flow at various stations of the turbine.

The gas flow in the scroll was assumed to be incompressible, and the scroll sections was constant and uniform. Although this solution is quite simple compared to the complicated nature of the three-dimensional flow problem, it does provide an approximately realistic gas flowfield into which the particles can be introduced.

The flow in the vortex regions were assumed to satisfy requirements of constant angular momentum and continuity. These flows, as well as the flow in all remaining regions of the turbine, are compressible.

Figure 3 illustrates the nozzle blade configuration that was selected for this analytical model turbine. There were 29 equally spaced blades. A velocity gradient technique was used to determine the irrotational two-dimensional flowfield through the passage. The solution steamlines based on this method are indicated.

In the rotor, the quasiorthogonal method[8] was used to determine the gas flow. There were 12 rotor blades in the model used in this study, with no splitter blades. The rotor tip

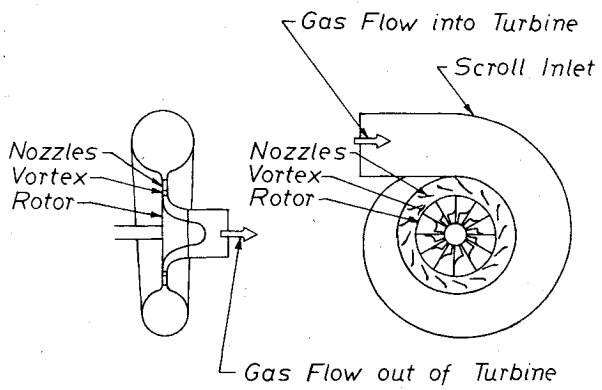

Fig. 1 Turbine model used in analytical study.

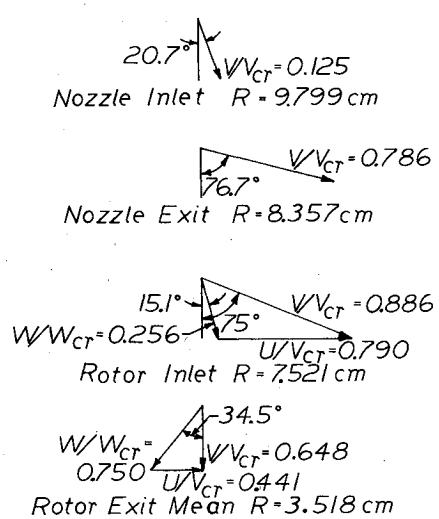

Fig. 2 Turbine velocity diagrams.

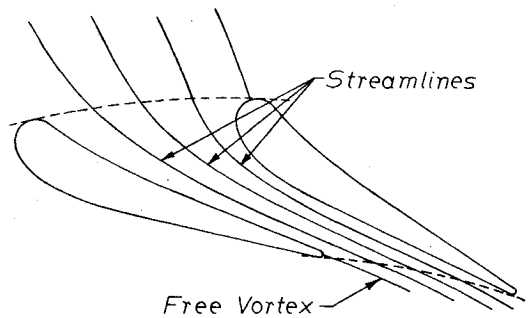

Fig. 3 Nozzle blades and flow.

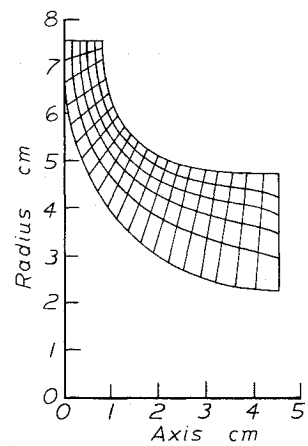

Fig. 4 Meridional view of rotor with streamlines and quasi-orthogonals.

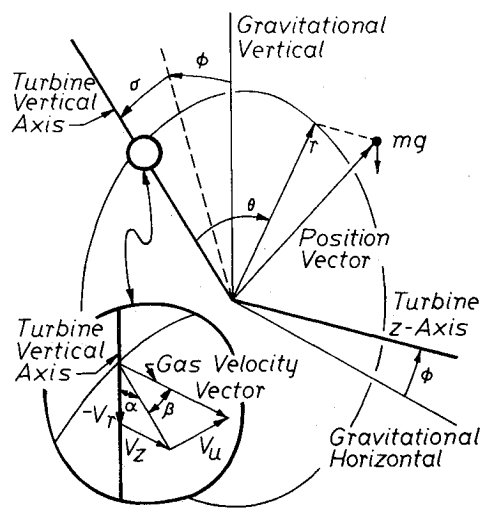

Fig. 5 Coordinate system.

radius was 7.52 cm. Figure 4 shows the solution strealines that occurred when this method was used. The solution is for an equivalent cold gas that has inlet stagnation conditions identical to standard sea level air.

Particle Motion Analysis

The analysis of particle trajectories in a fluid flowfield also requires the solution of the equations of motion of a particle immersed in the fluid. The equations of motion of a particle in a cylindrical coordinate system were used. The most general form of these equations are the ones of three-dimensional particle motion in a rotating reference frame. Figure 5 illustrates the coordinate system used throughout this paper.

Although gravitational forces can be neglected in most studies of particle motion, it was found that to neglect the gravitational acceleration could cause significant changes in the trajectories of particles in the scroll. Therefore, the particle weight was included in the general formulation of the equations.

Collecting the components of the acceleration, drag, and gravity forces through Newton's Law yields

$$\frac{\delta^2 r}{\delta t^2} - r\left(\frac{\delta\theta}{\delta t}\right)^2 - 2r\omega\frac{\delta\theta}{\delta t} - r\omega^2 = \frac{1}{2}\frac{\rho V^2 A C_D}{m}\frac{V_r}{|V|} - g\cos(\theta+\sigma) \tag{1}$$

$$r\frac{\delta^2\theta}{\delta t^2} + 2\frac{\delta r}{\delta t}\frac{\delta\theta}{\delta t} + 2\omega\frac{\delta r}{\delta t} = \frac{1}{2}\frac{\rho V^2 A C_D}{m}\frac{V_\theta}{|V|} + g\sin(\theta+\sigma) \tag{2}$$

$$\frac{\delta^2 z}{\delta t^2} = \frac{1}{2}\frac{\rho V^2 A C_D}{m}\frac{V_z}{|V|} - g\sin\theta \tag{3}$$

where

$$V = V_r e_r + V_\theta e_\theta + V_z e_z \tag{4}$$

The velocity vector given by Eq. (4) is the relative velocity of the gas with respect to the particle. The components of this relative velocity vector are

$$V_r = w_r - (\delta r/\delta t) \tag{5a}$$

$$V_\theta = w_\theta - r(\delta\theta/\delta t) \tag{5b}$$

$$V_z = w_z - (\delta z/\delta t) \tag{5c}$$

where w_r, w_θ, and w_z are, respectively, the radial, tangential, and axial components of the gas in the rotating reference frame in the most general case, and $\delta r/\delta t$, $r\delta\theta/\delta t$, and $\delta z/\delta t$ are, respectively, the radial, tangential, and axial velocity components of the particle in the rotating reference frame.

The drag coefficient of spherical particles is well-established experimentally over a large range of Reynold's numbers. A polynomial description of C_D was used in the numerical solution for the particle trajectories.

Similarity Parameter

Reference 7 describes the derivation and applicability of a similarity parameter that allows particles which follow a certain trajectory in a gas turbine to be related to different particles that will follow the same trajectory in a equivalent gas turbine. The similarity parameter is a characteristic length and is given by

$$S = (10/3)(\rho_p D_p/\rho_g) \tag{6}$$

This similarity parameter results from the matching of the inertial and drag forces acting on a particle.

The characteristic length S is a useful parameter because it allows the grouping of several variables that influence the trajectory of a particle into a single term. This allows a much wider range of applicability of trajectory data, such as result from equivalent cold flow turbines and cascade tunnels.

In the figures presented in this paper, the particle sizes are indicated in terms of diameters of SiO_2 particles. The trajectory associated with a certain diameter SiO_2 particle is the same trajectory followed by a different particle in a equivalent turbine, as long as the similarity parameter of the second particle is identical to the similarity parameter of the first particle. Letting the subscripts x, SiO_2, and Std refer to the terms associated, respectively, with the second particle, the SiO_2 particle, and the standard conditions of the model turbine, the characteristic lengths of each particle can be equated. When this is done and the terms have been rearranged, the diameter of the particle that will follow the same trajectory as the SiO_2 particle is found to be

$$D_{p_x} = X D_{p_{SiO_2}} \tag{7}$$

where

$$X = \frac{\rho_{p_{SiO_2}}\rho_{g_x}}{\rho_{p_x}\rho_{g_{Std}}} \tag{8}$$

As an example, suppose it is desired to predict the trajectory of an aluminum oxide particle in a real turbine. Suppose this turbine has a gas density 3 times that of standard sea level air. Since the density of aluminum oxide is 1.51 times the density of SiO_2, the value of X by Eq. (8) is 1.98.

Diameter Limit Parameter

Results presented later in this paper will show that the vortex region near the rotor tip tends to trap particles. This results because the particles that enter this vortex experience a centrifugal force that is greater than the aerodynamic force pushing the particle forward.

These two forces can be balanced to estimate the sizes of particles that can be expected to become trapped in this region. The required expression can be derived by considering a particle immersed in an inward moving vortex. If this particle is such that the aerodynamic force pushing the particle inward is identical to the centrifugal force pushing the particle outward, then the particle would move in an orbit about the axis. Figure 6a shows the general arrangement of gas and particle velocity vectors, whereas Fig. 6b illustrates the special case that occurs when the particle reaches a steady motion with equal centrifugal and radial drag forces. Noting that the vector difference between the gas velocity and the particle velocity is just the radial component of the gas velocity, $V = V_g\cos\beta_g e_r$, then the radial component of drag can be expressed as

$$D_r = 1/2 C_D \rho_g V_g{}^2 A_p \cos^2\beta_g \tag{9}$$

The centrifugal force pushing in the opposite direction is

$$F = \frac{m_p V_p{}^2}{r} = \frac{m_p V_g{}^2 \sin^2\beta_g}{r} \tag{10}$$

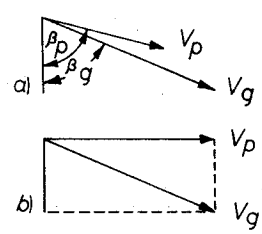

Fig. 6 Combined gas; particle velocity diagrams. a) General gas and particle diagrams. b) Diagram when particle has no radial velocity component.

Equating these two forces at the rotor tip and assuming that the particle is spherical yields, after rearranging,

$$P=\frac{3C_D}{8}=\frac{D_p\rho_p}{D_{tip}\rho_g}\tan^2\beta_g \qquad (11)$$

For large Reynolds numbers, the drag coefficient is constant at $C_D=0.4$. Using this, the dimensionless size parameter becomes a measure of whether a particle will move inward or outward near the rotor tip. Particles which have a size parameter $P<0.15$ will tend to move radially outward, thus failing to penetrate the rotor.

In the turbine model used in this paper, the size parameter can be applied to predict the sizes of particles that will not tend to penetrate the rotor. Doing so yields a SiO_2 particle size of approximately 0.7 μ in a more realistic turbine, having a gas density that is 2 to 3 times that of standard sea level air. This result is in agreement with the results presented in Ref. 1, where it was found that particles as small as 2–3 μ can be expected to cause a serious decrease in the engine operating lifetimes.

Trajectory Patterns

Three regions within the radial inflow turbine model were used to study the particle trajectories as they passed through the turbine. These regions included the scroll, the combined nozzle-vortex extending to the rotor tip, and the rotor. The trajectories presented resulted from analytically tracing the trajectories of selected particle sizes through the turbine. Particle sizes ranged from 4 to 370 μ. A complete collection of figures showing trajectories of most particle sizes is contained in Ref. 9.

The gas passing through a radial turbine first enters a scroll which is designed to distribute the air uniformly into the nozzles. Usually the velocities in the scroll are relatively small compared to the velocities in the vortex regions of the turbine.

Figure 7 shows the trajectories of 21-, 42-, and 83-μ particles in the scroll. The 21-μ particles did not strike the surfaces. These particles tended to move with the flow into the nozzle regions. The 42-μ particle moved outward from the axis and eventually struck the scroll's outer surface. Afterwards, these particles bounced repeatedly as they moved around the contour. They eventually struck the protion of the contour that is suppressed to prevent interference with the scroll inlet. Then they entered the nozzles at approximately the same location.

A similar trace is indicated for the 83-μ particle. This trajectory is truncated at the point where it crosses the trajectory of the 42-μ particle. Larger particles followed similar trajectories, except that they traveled longer distances between bounces. The results indicated in Fig. 7 are in general agreement with the experiments reported in Ref. 1.

In the nozzle-vortex region, relatively small particles with diameters of 8–21 μ will follow trajectories similar to those illustrated in Fig. 8. These trajectories have been extended from the trajectories that occurred in the scroll. As a convenience in presenting the results, the trajectories have been rotated artificially about the axis so that all particles appear to go through the same nozzle passage.

The 8-μ particles shown in Fig. 8 tend to move through the nozzle passages without striking the blade surfaces, but their motion is not identical to the gas flow. Therefore, some of these particles occasionally will bounce off the pressure surface of the nozzle blades. These trajectories are extended into the vortex and the figure shows that these particles moved through the vortex without entering the rotor. Eventually, the particles re-enter the nozzle region and strike the trailing edges of the blades.

Trajectory traces such as these also were done for particles having diameters of 4 μ. These traces indicated a tendency for these smaller particles to follow more closely the gas streamlines in the nozzle passages. The 4-μ particle trajectory showed the same tendency to pass into and out of the vortex without penetrating to the rotor tip.

The trajectories of particles with diameters of 83 μ are shown in Fig. 9. These larger particles are less influenced by the gas than the smaller particles, and the figure shows the tendency of the particle to travel from the pressure surface of the blade and impact on the suction surface of the blade. The impacts on both of these surfaces tend to be at even steeper angles, and most of the particles of this size that enter the turbine can be expected to strike the nozzle blade surfaces.

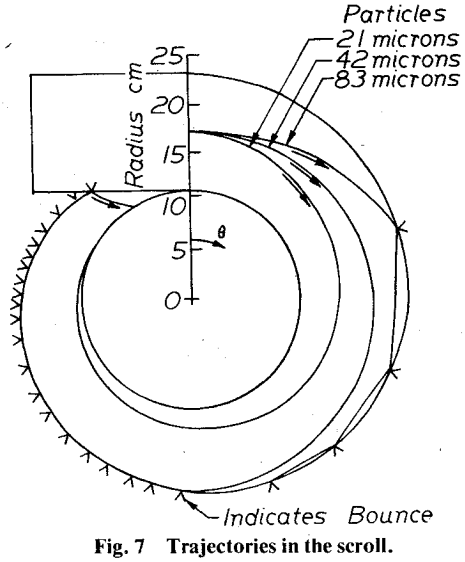

Fig. 7 Trajectories in the scroll.

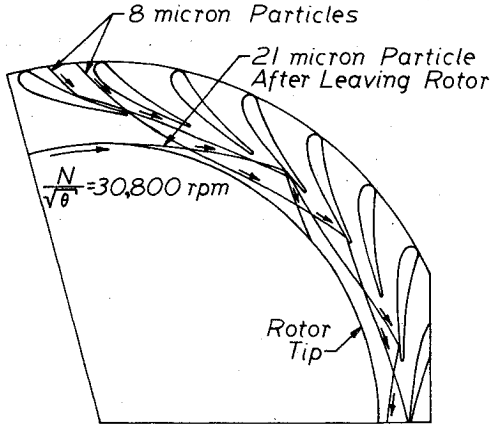

Fig. 8 Trajectories in the nozzles (8 μ particles).

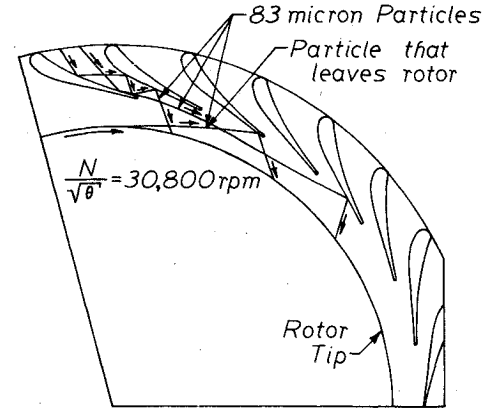

Fig. 9 Trajectories in the nozzles (83 μ particles).

Similar results are observed in trajectories for particles with diameters from 83 to 420 μ. All particles of this size range which enter the turbine can be expected to do erosion damage. The figure also illustrates that all of the particles with diameters of 83 μ or larger bounced off the nozzle trailing edges and into the rotor. The relatively slow moving particles then are struck by the rotor and pass out of the rotor with a velocity that is near the wheel speed. The trajectory that occurred for the 83-μ particle leaving the rotor was similar to the trajectory of the 21-μ particle shown in Fig. 8. These trajectories demonstrate the small influence that the gas has on these particles after they have been accelerated to the velocities of the rotor tip. Figure 10 shows the trajectories of particles that had diameters of 21 μ in the rotor. The figure illustrates the fact that these particles do not pass through the rotor. In addition, particles that enter near the suction surface of the rotor blade are struck by the rotor blade before they can be pushed out of the rotor by centrifugal forces. All the particles with diameters greater than 21 μ showed the same tendency, with the number of particles that are struck by the blade increasing as the particle size increases.

In the rotor, the trajectories of these larger particles that penetrate through the vortex and enter the rotor are modified as the rotor overtakes the slower moving particle. Because of the relatively slow velocity of the particle and the quite high velocity of the rotor blades, these impacts occur with relatively high incidence velocities and at relatively high incidence angles. After impact, the particle suddenly has a very large tangential velocity, and thus the centrifugal forces now are large enough to cause the particle to move radially outward. These particles continue their radial motion until they strike the nozzle trailing edges.

Experimental Results

To help understand these phenomena, an experimental radial inflow turbine configuration was designed to allow the use of high-speed motion pictures of the trajectories of particles in the radial turbine. These films illustrate the phenomenon of particles accumulating in the vortex region of the radial inflow turbine. Because of the relatively low performance levels of the experimental turbine, the films generally illustrate qualitatively the pheonomenon that occurs as particles enter the vortex and rotor tip region. The ratio of particle mass flow rate to total mass flow rate in these experiments was 0.63. This is a very high ratio and would be experienced in only the most extreme conditions in the field.

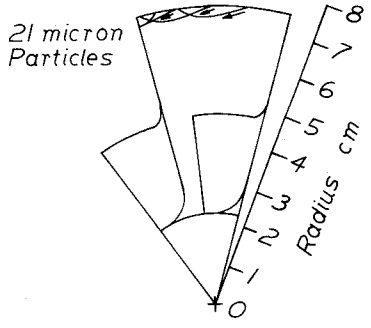

Fig. 10 Axial view of rotor with respect to rotating reference frame.

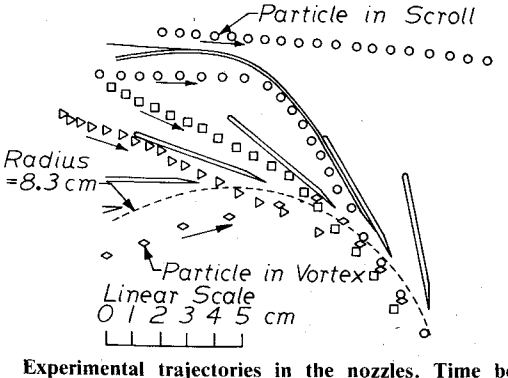

Fig. 11 Experimental trajectories in the nozzles. Time between points = 3.77×10^{-4} sec. Equivalent 400 μ SiO_2 particles.

One of the first things that was noted in this study was that all of the particles appear to move all the way around the scroll before they enter the last couple of passages of the nozzles. However, this is in agreement with the analytical results, because particles that are large enough to be recorded on film are greater than 42 μ.

A second observation that agrees with the analytical results is the motion of the particles in the free vortex region of the turbine. These particles were observed to accumulate in this region of the flow and to strike the trailing edges of the nozzle blades with a large number of moderate-angle impacts.

Another observation is that particles accumulate in the vortex region. Less than a second after the particle flow was started, there were so many particles that a ring of high particle density was formed. Such an event occurring in a real turbine operating in a very dusty environment would cause an immediate drop in the turbine performance.

Several films were taken with the flat plate rotor installed. These films show, in addition to the previous observations, the apparently almost perpendicular impacts that occur on the rotor tips. This is in agreement with the results that were predicted by the analytical study of the particle trajectories in the rotor. Because the particles used in these films had rather high characteristic lengths, they would be expected to impact on the rotor in this way.

Another film was used to accumulate data on the trajectories of particles through the nozzle regions of the turbine. The test configurations did not use a rotor in this particular experiment and the velocity at the nozzle exit was 0.320 times the critical velocity and had an angle of about 70° . The data accumulated included plots of several trajectories as the particles entered the turbine configuration.

Figure 11 illustrates the trajectories that occur in the nozzles at the end of the scroll region of the experimental turbine. These particles were 2000 μ, having a specific gravity of about 1.1. Based on the inlet conditions to the turbine, the corresponding SiO_2 particle size is approximately 400 μ. The time between points is indicated to clarify the velocity measurements that can be made from trajectory plots such as these.

These trajectories are typical of those that occurred during the movie. The increasing distance between the points as the particle moves through the nozzles and into the vortex illustrates the acceleration in the tangential direction. These trajectories are different from those that occurred in the analytical work because the nozzle configuration in the two turbines are different. This shows the influence which nozzle design can have on the erosion in these regions. This figure also shows a particle in the scroll. This particle is accelerating and during the time that it was observed, it accelerated uniformly from 85 to 98% of the gas velocity.

Summary and Conclusions

The purpose of this paper has been to describe the trajectories of erosive sizes of particles in radial inflow turbines. The forces that influence the motion of a particle as it passes through the vortex regions of a radial inflow turbine were considered. These forces are primarily the radial component of the aerodynamic drag force and the centrifugal force. By balancing these two forces, a dimensionless parameter has been derived which will predict the sizes of particles that can be expected to cause erosion damage within a radial turbine.

The study of trajectory patterns in the scroll reveals that particles with diameters greater than 42 μ tended to move radially outward and to strike the outer edges of the scroll.

Most of these particles then impact with low-velocity, moderate-angle impacts on the portion of the scroll that is suppressed to prevent interference with the scroll inlet. This relatively small area of the scroll contour would be subject to a more severe erosion problem.

Investigation of the trajectories in the nozzles indicated that most of the particles with diameters greater than 42 μ would cause erosion on a few of the nozzle blade passages near the scroll exit. These particles appear to strike the pressure and suction surfaces of the nozzle blades with low-velocity and moderate-angle impacts. The study also indicated that the trailing edges of the nozzle blades would be subjected to a very large number of high-velocity, moderate-angle impacts by any particles with diameters greater than about 1 μ. This results because these particles tend to accumulate in the vortex region, and the larger particles that enter the rotor are struck by it and accelerated to very high tangential velocities.

The study indicated that the particles with diameters greater than about 21 μ tended to enter the rotor passages with velocities about 50% of the gas velocity at the rotor inlet, but were overtaken quickly by the rotor and suddenly accelerated to very high tangential velocities. These particles struck the rotor tip with very high velocities, with respect to the rotor tip, and with very high incidence angles. After leaving the rotor, these particles travel to the nozzle blade trailing edges where they impact with very high velocities and moderate angles. This impact slows the particles and deflects them into the rotor where the phenomena starts repeating itself. Thus, particles greater than 21 μ can be expected to cause a significant amount of erosion.

As the particle size decreases, the particles tend to follow the streamline of the flow. This action tends to prevent many of the particles from striking the rotor blade surfaces. Particles with diameters approximately 1 μ or less will pass through the rotor without causing erosion damage.

References

[1]Montgomery, J. E. and Clark, J. M., "Dust Erosion Parameters for a Gas Turbine," SAE Paper No. 538, June 1962.

[2]Shoemaker, H. E. and Shumate, C. P., "Techniques for Reducing Sand and Dust Erosion in Small Gas Turbine Engines," SAE Paper No. 700706, Sept. 1970.

[3]Soo, S. L., "Gas Dynamic Processes Involving Suspended Solids," *AIChE Journal*, Vol. 7, Sept. 1961, pp. 384-391.

[4]Bailey, W. S., Nilsen, R. A., Serra, R. A., and Zipnik, T. F., "Gas Particle Flow in an Axisymmetric Nozzle," *ARS Journal*, Vol. 31, June 1961, pp. 793-798.

[5]Tabakoff, W. and Hussein, M. F., "Trajectories of Particles Suspended in Fluid Flow through Cascades," *Journal of Aircraft*, Vol. 8, Jan 1971, pp. 60-62.

[6]Grant, G. and Tabakoff, W., "Erosion Prediction in Turbomachinery Resulting from Environmental Solid Particles," *Journal of Aircraft*, Vol. 12, May 1975, pp. 471-478.

[7]Clevenger, W. B., and Tabakoff, W., "Similarity Parameters for Comparing Erosive Particle Trajectories in Hot Air and Cold Air Radial Inflow Turbines," *Transactions of the ASME, Journal of Engineering for Power*, Vol. 96, Oct. 1974, pp. 358-364.

[8]Katsanis, T., "Use of Arbitrary Quasi-Orthogonals for Calculating Flow Distribution in the Meridional Plane of a Turbomachine," NASA, TN D-2546, 1964.

[9]Clevenger, W. B. and Tabakoff, W., "Erosion in Radial Inflow Turbines—Volume III," NASA, CR134700, Aug. 1974.